PRAMANA — journal of physics
© Indian Academy of Sciences
Vol. 83, No. 4
October 2014
pp. 533–543

Capture cross-section and rate of the ^{14}C(n, γ)^{15}C reaction from the Coulomb dissociation of ^{15}C

SHUBHCHINTAK, NEELAM and R CHATTERJEE*

Department of Physics, Indian Institute of Technology Roorkee, Roorkee 247 667, India
*Corresponding author. E-mail: rcfphfph@iitr.ac.in

MS received 28 October 2013; revised 16 January 2014; accepted 4 February 2014
DOI: 10.1007/s12043-014-0798-2; ***e*Publication:** 13 August 2014

Abstract. We calculate the Coulomb dissociation of ^{15}C on a Pb target at 68 MeV/u incident beam energy within the fully quantum mechanical distorted wave Born approximation formalism of breakup reactions. The capture cross-section and the subsequent rate of the ^{14}C(n, γ)^{15}C reaction are calculated from the photodisintegration of ^{15}C, using the principle of detailed balance. Our theoretical model is free from the uncertainties associated with the multipole strength distributions of the projectile.

Keywords. Coulomb dissociation; radiative capture; reaction rate.

PACS Nos 24.10.−i; 24.50.+g; 25.40.Lw; 25.60.Tv

1. Introduction

The radiative neutron capture (n, γ) process constitutes an important nucleosynthesis path in the neutron-rich region of the nuclear chart. However, it is a challenge both from theoretical and experimental points of view, given that in many cases one has to deal with nuclei away from the valley of stability and cross-sections have to be measured at very low energies relevant for stellar processes. Often, when direct measurements are difficult or in some cases currently not feasible, one resorts to indirect methods like the Coulomb dissociation method where equivalent information can be extracted by performing measurements at higher beam energies.

However, there are a very few neutron capture reactions for which both direct and indirect measurements of the cross-sections have been possible. The ^{14}C(n, γ)^{15}C radiative capture reaction is one such example. As discussed by Wiescher *et al* [1], it plays an important role in the neutron-induced CNO cycle,

$$^{12}\mathrm{C}(n,\gamma)^{13}\mathrm{C}(n,\gamma)^{14}\mathrm{C}(n,\gamma)^{15}\mathrm{C}(\beta^-)^{15}\mathrm{N}(n,\gamma)^{16}\mathrm{N}(\beta^-)^{16}\mathrm{O}(n,\gamma)^{17}\mathrm{O}(n,\alpha)^{14}\mathrm{C},$$

which occurs in the helium burning layers of asymptotic giant branch stars. Being the slowest in the cycle, its rate is important to predict the abundance of ^{14}C given that it is one of the possible paths by which ^{14}C can decay. Another importance of this reaction is in inhomogeneous Big Bang model [2], which offers possible ways to bridge $A = 8$ gap and hence the production of elements with $A \geq 12$. The suggested reaction sequence in the neutron-rich zone is

$$^{7}\text{Li}(n,\gamma)^{8}\text{Li}(\alpha,n)^{11}\text{B}(n,\gamma)^{12}\text{B}(\beta^{-})^{12}\text{C}.$$

Then the subsequent neutron capture over ^{12}C and ^{13}C leads to the production of ^{14}C, half-life of which (5700 ± 30 years) is longer than the time-scale of Big Bang nucleosynthesis. So, ^{14}C is considered to be a seed nucleus for the production of heavier nuclei with $A \geq 20$, where $^{14}\text{C}(n,\gamma)^{15}\text{C}$ competes with alpha, proton and deuteron capture reactions on ^{14}C [3,4].

Experimental efforts to measure the $^{14}\text{C}(n,\gamma)^{15}\text{C}$ cross-section via both the direct and indirect methods started during the early nineties. However, there are disagreements in the extracted values of the cross-sections, especially at very low energies. The first direct experiment to measure the (n,γ) cross-section of ^{14}C was performed by Beer *et al* [5]. The extracted Maxwellian averaged capture cross-section (MACS) was 1.72 ± 0.43 μb at 23.3 keV. This was very small compared to MACS extracted from another direct experiment by Reifarth *et al* [6], who found it to be 7.1 ± 0.5 μb. Horváth *et al* [7] extracted the value 2.6 ± 0.9 μb from the experiment based on Coulomb breakup of ^{15}C on Pb at 35 MeV/u. Another Coulomb breakup experiment was performed at GSI [8,9] at high energy (605 MeV/u) and the extracted value of capture cross-section was 4.1 ± 0.6 μb. Recently, Nakamura *et al* [10] also performed a Coulomb breakup experiment at 68 MeV/u beam energy to calculate the cross-section of (n,γ) reaction. The MACS value extracted at 23.3 keV was 6.1 ± 0.5 μb.

The theoretical calculations by Wiescher *et al* [2], based on the direct capture model [11], predicted the value of capture cross-section to be 5.1 μb. This value was in good agreement with the value calculated from other theoretical models like folding model [12] and the microscopic cluster model [13]. In ref. [14], an indirect method based on mirror symmetry was used to extract the (n,γ) cross-section. Their value (5.3 ± 0.3 μb) was also consistent with that of ref. [2]. Recently, a continuum discretized coupled channel calculation [15] and also a semiclassical model based on the dynamical description of diffraction dissociation of weakly bound nuclei [16] have also been reported to calculate the cross-section of $^{14}\text{C}(n,\gamma)^{15}\text{C}$.

With this background, we present a fully quantum mechanical calculation of the Coulomb breakup of ^{15}C on Pb at 68 MeV/u beam energy within the aegis of post-form finite range distorted wave Born approximation (FRDWBA) and then extract the $^{14}\text{C}(n,\gamma)^{15}\text{C}$ radiative capture cross-section and the reaction rate at relevant stellar temperatures. The theory includes the electromagnetic interaction between the fragments and the target to all orders. Furthermore, the breakup contribution from the entire non-resonant continuum (corresponding to all multipoles and relative orbital angular momentum between the fragments) are also accounted for. The uncertainties associated with multipole strength distributions in many other formalisms are also avoided as one needs only the ground-state wave function of the projectile as an input. The analytic nature of this theory stems from the fact that pure Coulomb wave functions are used in the calculation and that the dynamics can be analytically evaluated. The first application [17] of this formalism to nuclear astrophysics was on the Coulomb dissociation of ^{9}Li on heavy targets to calculate the ^{9}Li$(n, \gamma)^{9}$Li capture cross-section. We would therefore like to apply the formalism to the case of ^{14}C$(n, \gamma)^{15}$C for two reasons: first to take advantage of the analytic nature and secondly to bring into focus a slight discrepancy in the peak position of the relative energy spectrum in the Coulomb breakup of ^{15}C at two different beam energies [8,10].

The paper is organized in the following way. In §2, we present a brief formalism of the Coulomb breakup process and the capture cross-section. Our results are presented in §3, where we discuss the capture cross-section and rate of the ^{14}C$(n, \gamma)^{15}$C reaction from the Coulomb dissociation of ^{15}C and finally in §4, we present our conclusions.

2. Formalism

We consider the elastic breakup of a two-body composite projectile a in the Coulomb field of the target t as: $a + t \to b + c + t$, where the projectile a breaks up into fragments b (charged) and c (uncharged). The Jacobi coordinate system adopted is shown in figure 1.

The position vectors $\mathbf{r}_1$, $\mathbf{r}_i$, $\mathbf{r}_c$ and $\mathbf{r}$ satisfy the following relations:

$$\mathbf{r} = \mathbf{r}_i - \alpha \mathbf{r}_1; \quad \mathbf{r}_c = \gamma \mathbf{r}_1 + \delta \mathbf{r}_i.$$

α, γ and δ are the mass factors, given by

$$\alpha = \frac{m_c}{m_c + m_b}; \qquad \delta = \frac{m_t}{m_b + m_t}; \qquad \gamma = (1 - \alpha\delta),$$

where m_b, m_c and m_t are the masses of fragments b, c and t, respectively.

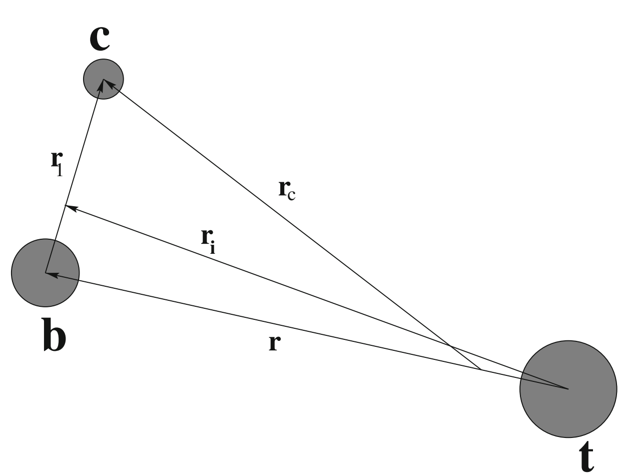

Figure 1. The three-body Jacobi coordinate system.

The relative energy spectra for the reaction is given by

$$\frac{\mathrm{d}\sigma}{\mathrm{d}E_{\mathrm{rel}}} = \int_{\Omega_{bc}\Omega_{at}} \mathrm{d}\Omega_{bc}\mathrm{d}\Omega_{at} \times \sum_{lm} \frac{1}{(2l+1)} |\beta_{lm}|^2 \frac{2\pi}{\hbar v_{at}} \frac{\mu_{bc}\mu_{at} p_{bc} p_{at}}{h^6}, \tag{1}$$

where E_{rel} is the b–c relative energy in the final channel, v_{at} is the a–t relative velocity in the initial channel, Ω_{bc} and Ω_{at} are solid angles, μ_{bc} and μ_{at} are the reduced masses and p_{bc} and p_{at} are linear momenta of the b–c and a–t systems, respectively. β_{lm} is the reduced amplitude in post-form FRDWBA, given by

$$\hat{l}\beta_{lm}(\mathbf{q}_b, \mathbf{q}_c; \mathbf{q}_a) = \int\int \mathrm{d}\mathbf{r}_1 \mathrm{d}\mathbf{r}_i \chi_b^{(-)*}(\mathbf{q}_b, \mathbf{r})\chi_c^{(-)*}(\mathbf{q}_c, \mathbf{r}_c) \times V_{bc}(\mathbf{r}_1)\phi_a^{lm}(\mathbf{r}_1)\chi_a^{(+)*}(\mathbf{q}_a, \mathbf{r}_i), \tag{2}$$

where $\hat{l} = \sqrt{2l+1}$, $\mathbf{q}_b$, $\mathbf{q}_c$ and $\mathbf{q}_a$ are the wave vectors of b, c and a corresponding to Jacobi vectors $\mathbf{r}$, $\mathbf{r}_c$ and $\mathbf{r}_1$, respectively, V_{bc} is the interaction between b and c in the initial channel, $\phi_a^{lm}(\mathbf{r}_1)$ is the ground state wave function of the projectile with relative orbital angular momentum state l and projection m. $\chi^{(-)}$s are the Coulomb distorted waves for relative motions of b and c with respect to t and the centre of mass (c.m.) of the b–t system, respectively, with incoming wave boundary conditions. One replaces $\chi_c^{(-)}$ by a plane-wave as there would be no Coulomb interaction between c (uncharged) and t. $\chi^{(+)}(\mathbf{q}_a, \mathbf{r}_i)$ is the Coulomb distorted wave for the scattering of the c.m. of the projectile a with respect to the target with outgoing wave boundary conditions.

β_{lm} (eq. (2)) is a six-dimensional integral, which can be simplified by using the local momentum approximation [18], whereby it reduces to two three-dimensional integrals, one giving the structure information and the other involving the dynamics of the reaction, which in turn can be evaluated analytically in terms of the Bremsstrahlung integral [19]. For the validity of the local momentum approximation in our case one is referred to Appendix A and for more discussions on the approximation to refs [20–22].

The relative energy spectra (eq. (1)) is then related [23] to the photodisintegration cross-section ($\sigma_{\gamma,n}^{\pi\lambda}$) as

$$\frac{\mathrm{d}\sigma}{\mathrm{d}E_{\mathrm{rel}}} = \frac{1}{E_\gamma} \sum_{\pi\lambda} \sigma_{\gamma,n}^{\pi\lambda} n_{\pi\lambda}, \tag{3}$$

where π stands for either electric or magnetic transition of multipolarity λ, $n_{\pi\lambda}$ is the equivalent photon number and depends on the a–t system [23] and $E_\gamma = E_{\mathrm{rel}} + Q$ is the photon energy with Q as the Q-value of the reaction.

Now, if a single multipolarity dominates, which is the case for the breakup of ^{15}C [14,24], then one can estimate the photodisintegration cross-section as

$$\sigma_{\gamma,n}^{\pi\lambda} = \frac{E_\gamma}{n_{\pi\lambda}} \frac{\mathrm{d}\sigma}{\mathrm{d}E_{\mathrm{rel}}}. \tag{4}$$

The equivalent photon number $n_{\pi\lambda}$ is calculated as

$$n_{\pi\lambda} = \int_0^{\theta_{\mathrm{gz}}} \frac{\mathrm{d}n_{\pi\lambda}}{\mathrm{d}\Omega_{at}} \mathrm{d}\Omega_{at}, \tag{5}$$

where $\theta_{\rm gz}$ is the grazing angle for the scattering and $\mathrm{d}n_{\pi\lambda}/\mathrm{d}\Omega_{at}$ is the equivalent photon number per unit solid angle. For $E1$ transition (as in the present case), it is given by [25]

$$\frac{\mathrm{d}n_{E1}}{\mathrm{d}\Omega_{at}} = \frac{Z_t^2\alpha}{4\pi^2}\left(\frac{c}{v_{at}}\right)^2 \epsilon^4\eta^2 \mathrm{e}^{-\pi\eta}\left\{\frac{1}{\gamma^2}\frac{\epsilon^2-1}{\epsilon^2}[K_{i\eta}(\epsilon\eta)]^2 + [K'_{i\eta}(\epsilon\eta)]^2\right\}, \quad (6)$$

where $\eta = E_\gamma a/\hbar v_{at}\gamma$, with $a = Z_a Z_t e^2/\mu_{at} v_{at}^2$ being the half distance of the closest approach in the head on collision. $\alpha = e^2/\hbar c$, $K_{i\eta}(y)$ are the modified Bessel functions and $K'_{i\eta}(y)$ are the derivative of $K_{i\eta}(y)$ with respect to y. Further, ϵ is the eccentricity parameter and it is related to the scattering angle θ_{at} as $\epsilon = 1/\sin(\theta_{at}/2)$. The relativistic factor γ is given by $\gamma = 1/\sqrt{1-v_{at}^2/c^2}$. At this point it may be worthwhile to reiterate that we have directly used the form of eq. (6) in eq. (5). Several forms of n_{E1} exist in the literature which essentially can be traced to eq. (6) being reduced to its pure non-relativistic and relativistic forms for $\gamma \approx 1$ and $\gamma \gg 1, \epsilon \gg 1$, respectively (for more details, one is referred to refs [23,25,26].

The radiative capture cross-section $\sigma_{n,\gamma}$ can then be calculated utilizing the principle of detailed balance,

$$\sigma_{n,\gamma} = \frac{2(2j_a+1)}{(2j_b+1)(2j_c+1)}\frac{k_\gamma^2}{k_{bc}^2}\sigma_{\gamma,n}^{\pi\lambda}, \quad (7)$$

where j_a, j_b and j_c are the spins of particles a, b and c, respectively. k_γ and k_{bc} are the wave numbers of the photon and that of relative motion between b and c, respectively.

3. Results and discussions

3.1 *Structure of ^{15}C*

^{15}C has a relatively large value for the one-neutron separation energy (1.218 MeV) compared to halo nuclei like ^{19}C and ^{11}Be. It has a ground-state spin-parity of $1/2^+$ and therefore we consider it primarily to be a $1s_{1/2}$ neutron coupled to a ^{14}C(0^+) core. The single-particle relative motion wave function for neutron is constructed by assuming a Woods–Saxon interaction between the valence neutron and the charged core whose depth is adjusted to reproduce the binding energy. The depth turns out to be 55.40 MeV for radius and diffuseness parameters of 1.223 fm and 0.5 fm (same as ref. [10]), respectively. We also checked our calculations by including a spin-orbit term in potential following ref. [16], but then it does not seem to have any effect on our results.

3.2 *Relative energy spectra and the neutron capture cross-section*

In figure 2, we show the relative energy spectra in the pure Coulomb breakup of ^{15}C on a Pb target at 68 MeV/u beam energy. The centre of mass angle in this case has been integrated from 0° to 2.1°, in order to compare it with experimental data [10] of the same limit. We normalize our calculations to the data peak, in lieu of the spectroscopic factor or to account for any possible detector efficiency.

It is interesting to note that for the RIKEN experiment [10] (incident beam energy = 68 MeV/u), the peak of the relative energy spectra comes at a relative energy of 0.55 MeV or a little more. In the GSI experiment [8] (incident beam energy = 605 MeV/u), the peak of the excitation energy spectra is at an excitation energy of 1.67 MeV. So if one subtracts the one-neutron separation energy of ^{15}C from this energy, one would correspondingly expect the relative energy spectra to peak at 0.45 MeV. This peak position is slightly different from the experiment at 68 MeV/u. However, it is in agreement with what our calculations suggest. This can be seen in the inset of figure 2, which shows the GSI data in comparison with our calculation (at 68 Mev/u), which has been normalized to the peak of the high-energy data.

As one would not expect the peak position of the relative energy spectra to change with incident beam energies, this slight discrepancy in the peak position between these experiments needs to investigated.

The relative energy spectra is then used to calculate the photodisintegration cross-section (eq. (4)) and subsequently the $^{14}\mathrm{C}(n,\gamma)^{15}\mathrm{C}$ radiative capture cross-section (eq. (6)). Of course, to ensure the applicability of eq. (4), we have checked that the breakup is dominated by the electric dipole contribution [14,24]. In fact, estimates of the dipole contribution and its dominance in the breakup of weakly bound nuclei have also been discussed in refs [27–29] by simple analytic arguments in the extreme single-particle model.

In figure 3, we show our $^{14}\mathrm{C}(n,\gamma)^{15}\mathrm{C}$ radiative capture cross-section (solid line) as a function of the centre of mass energy ($E_{\mathrm{c.m.}}$) and compare it with the experimental data from two different experiments. The solid black circles ($E_{\mathrm{c.m.}}$ = 0.05–3.0) are the data

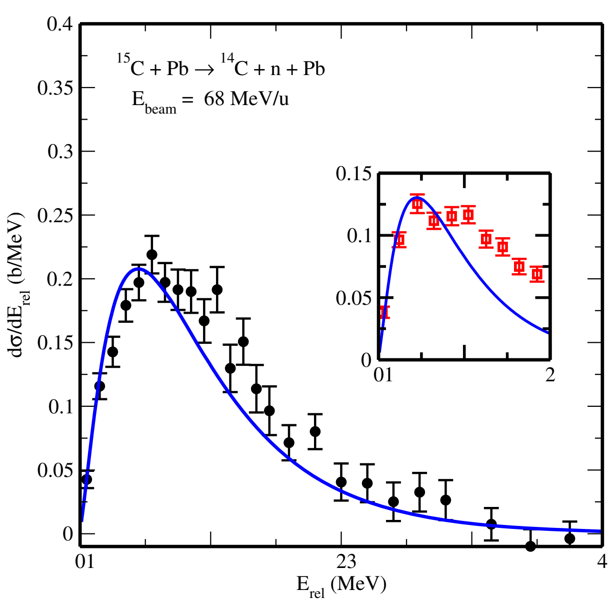

Figure 2. Relative energy spectra in the Coulomb breakup of ^{15}C on a Pb target at 68 MeV/u incident beam energy. The centre of mass angle has been integrated from 0°–2.1°. Experimental data are from ref. [10]. The inset shows the data from ref. [8] at 605 MeV/u, compared with the same calculation (for more details, see text).

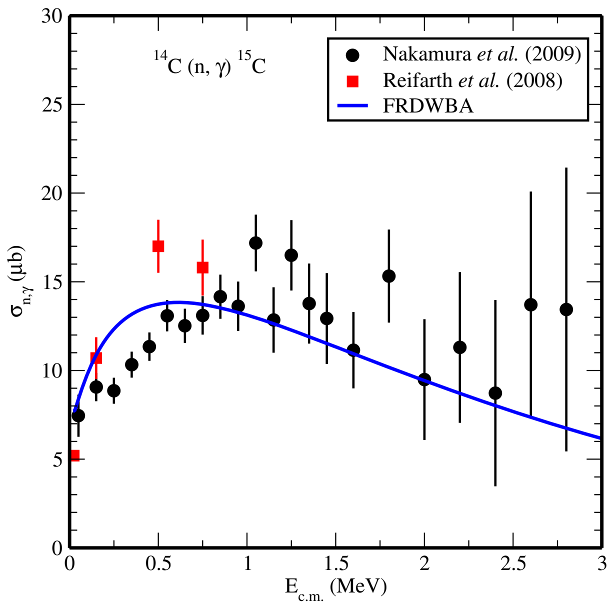

Figure 3. Neutron capture cross-section of ^{14}C (solid line) compared with direct measurements (solid squares), from refs [6,30] and indirect measurements (solid circles) based on Coulomb dissociation data, from ref. [10].

from ref. [10] where neutron capture cross-sections are calculated from the Coulomb dissociation method. The low energy direct measurements ranging from $E_{\text{c.m.}} = 0.02$–0.8 MeV (solid squares), are from refs [6,30]. As mentioned earlier, this is one of the few cases where data exist for both direct and indirect measurements for the same reaction and except for a small region around $E_{\text{c.m.}} = 0.5$ MeV, we see a reasonably good agreement between these experiments. Our calculated capture cross-section at $E_{\text{c.m.}} = 23.3$ keV is 7.71 μb which also compares well with that of Descouvemont (see refs [6,13]).

3.3 *Reaction rate*

As mentioned earlier, $^{14}\text{C}(n,\gamma)^{15}\text{C}$ is in direct competition with proton, deuteron and α capture on ^{14}C for the production of heavier isotopes with $A \geq 20$. Earlier it was suggested by Applegate *et al* [3], that once ^{14}C is formed, further production of heavier elements is ignited via the (α,γ) reaction. Kajino *et al* [31], on the other hand claimed that due to high neutron abundance, (n,γ) is a significant reaction path after ^{14}C formation. Furthermore, in ref. [2], the calculated rates indicate that $^{14}\text{C}(p,\gamma)^{15}\text{N}$ reaction is important for temperature $T_9 > 0.8$ (temperature in units of 10^9 K). Contradicting all these, Kawano *et al* [32], on the basis of their calculations suggested that $^{14}\text{C}(d,n)^{15}\text{N}$ reaction plays a major role in the destruction of ^{14}C. So, it is important to find the rate of $^{14}\text{C}(n,\gamma)^{15}\text{C}$ reaction at various temperatures, especially in the temperature range important for the inhomogeneous Big Bang model.

The reaction rate per mole [33], $N_A\langle\sigma v\rangle$ (N_A being Avogadro constant), is related to the neutron capture cross-section $\sigma_{n,\gamma}(E)$ by

$$N_A\langle\sigma v\rangle = N_A\sqrt{\frac{8}{(kT)^3\pi\mu_{bc}}}\int_0^\infty \sigma_{n,\gamma}(E)E\exp\left(-\frac{E}{kT}\right)\mathrm{d}E, \tag{8}$$

where k is the Boltzmann constant, T is the temperature in Kelvin (K) and μ_{bc} is the reduced mass of the ^{14}C$-n$ system. The energy integration in our case is preformed from 0.02 to 3 MeV, consistent with the energy range shown in figure 3.

In figure 4, we compare our calculated reaction rate (solid line) with those obtained earlier. The dashed and dot–dashed lines are theoretical predictions from refs [2] and [13], respectively. The starred, dotted and squared lines are evaluations based on various experimental estimates of the capture cross-section from refs [5–7], respectively.

It would be interesting now to compare the ^{14}C$(p,\gamma)^{15}$N reaction rate (line with triangles) calculated by Kawano *et al* [32], in the same graph. Our calculations show that ^{14}C$(n,\gamma)^{15}$C reaction will dominate over ^{14}C$(p,\gamma)^{15}$N for temperature $T_9 < 1.4$. This would imply that in the temperature range relevant for inhomogeneous Big Bang model ($T_9 = 0.2-1.2$), ^{14}C would be destroyed more by the (n,γ) process than by the (p,γ) process. This conclusion is also consistent with the rate from Reifarth *et al*, whose rate compare quite well with our theoretical estimates in the temperature range mentioned above. We wish to stress that our calculated rate is based on capture cross-sections estimated at very low energies to comparably higher energies and compared with both direct and indirect measurements.

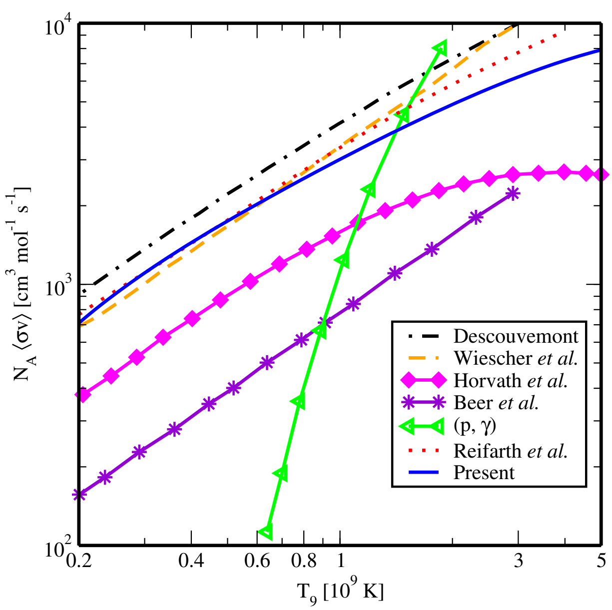

Figure 4. Calculated ^{14}C$(n,\gamma)^{15}$C reaction rate (solid line), compared with the other theoretical predictions and evaluations based on various experimental estimates of the capture cross-section (for more details, see text).

4. Conclusions

In conclusion, we have calculated the ^{14}C$(n,\gamma)^{15}$C radiative capture cross-section and the associated reaction rate by studying the Coulomb dissociation of ^{15}C on Pb at 68 MeV/u, within the fully quantum mechanical post-form distorted wave Born approximation. The entire non-resonant continuum is accounted for in the theory. We calculate the relative energy spectra in the breakup of ^{15}C on Pb at 68 MeV/u and discuss it in comparison with the available data [10]. However, one must add that for a more universal application of our theory, especially at very high beam energies, relativistic effects need to be taken into consideration. The local momentum approximation is also a price one has to pay to retain the analytic nature of the dynamics part of the formalism. In fact, efforts are on to overcome this problem, especially for neutron halo nuclei.

The neutron capture cross-section is then calculated from the photodisintegration cross-section of ^{15}C, using the principle of detailed balance. Comparison with available data from both the direct and indirect measurements is done for a wide energy range. While our calculation is in good agreement with both data, we wish to point out that at $E_{\rm c.m.} = 0.5$ MeV, there are some disagreements between the direct measurements and those extracted from the Coulomb dissociation data. As this is the region where the capture cross-section is expected to be maximum, it would be useful to experimentally investigate this region in more details.

We also calculate the ^{14}C$(n,\gamma)^{15}$C reaction rate per mole as a function of temperature. They are in good agreement with that evaluated from the direct measurement of the capture cross-section [6] especially for $T_9 < 1$. Our results also show that ^{14}C$(n,\gamma)^{15}$C reaction will dominate over ^{14}C$(p,\gamma)^{15}$N for temperature $T_9 < 1.4$.

Acknowledgements

This text presents results from research supported by the Department of Science and Technology, Govt. of India, (SR/S2/HEP-040/2012). The authors would like to thank Prof. T Nakamura for sending them the data of ref. [10] in a tabular form. Support from MHRD grants, Govt. of India, to Shubhchintak and Neelam are gratefully acknowledged.

Appendix A. Validity of the local momentum approximation

The factorization of the breakup amplitude (eq. (2)) is affected with the help of the local momentum approximation [20–22], on the outgoing charged fragment b. Essentially, one uses the Taylor expansion of $\chi_b^{(-)*}(\mathbf{q}_b, \mathbf{r})$ about $\mathbf{r}_{\rm i}$, which is exact and helps in the separation of variables $\mathbf{r}_{\rm i}$ and $\mathbf{r_1}$,

$$\chi_b^{(-)}(\mathbf{q}_b, \mathbf{r}) = \mathrm{e}^{-\alpha \mathbf{r}_1 . \nabla_{r_i}} \chi_b^{(-)}(\mathbf{q}_b, \mathbf{r}_{\rm i}). \tag{A.1}$$

The approximation involves the replacement of del-operator by an effective local momentum, $\mathbf{K}(= -i\nabla_{\mathbf{r}_i})$, whose magnitude is given by

$$\mathbf{K} = \sqrt{\frac{2\mu_{bt}}{\hbar^2}(E_{bt} - V(R))}, \tag{A.2}$$

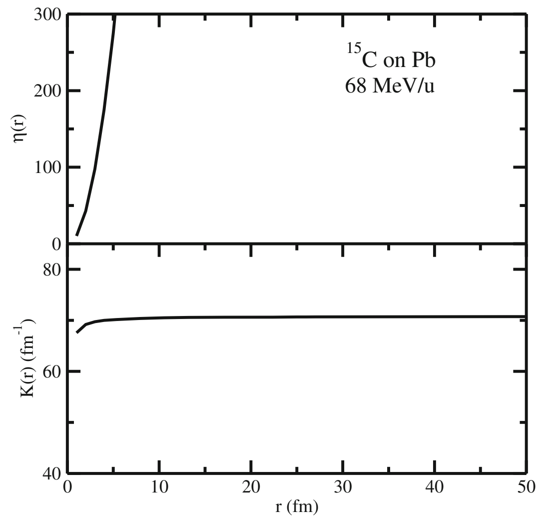

Figure 5. Variation of $\eta(r)$ (upper half) and $K(r)$ (lower half) with r for the Coulomb breakup of ^{15}C.

where μ_{bt} is the reduced mass of the b–t system, E_{bt} is the energy of particle b relative to the target in the c.m. system and $V(R)$ is the Coulomb potential between b and the target at a distance R. Thus, the local momentum $\mathbf{K}$ is evaluated at some distance R (10 fm, in our case) and its magnitude is held fixed for all the values of $\mathbf{r}$. The direction of $\mathbf{K}$ is taken as that of the outgoing fragment b. The condition of validity (see eg. [20]) is that the quantity

$$\eta(r) = \frac{\frac{1}{2}K(r)}{|\mathrm{d}K(r)/\mathrm{d}r|}, \tag{A.3}$$

calculated at some representative distance R should be more than the projectile radius, r_a.

To check the validity of the approximation, in figure 5 we show the variation of $\eta(r)$ (upper half) and $K(r)$ (the magnitude of the local momentum) (lower half) as a function of r, for the Coulomb breakup reaction $^{15}\mathrm{C} + \mathrm{Pb} \to {}^{14}\mathrm{C} + n + \mathrm{Pb}$ at the beam energy of 68 MeV/u. At $r = 10$ fm, $\eta(r) \gg r_a = 3.12$ fm, the projectile r.m.s. radius.

References

[1] M Wiescher, J Görres and H Schatz, *J. Phys. G* **25**, R133 (1999)
[2] M Wiescher, J Görres and F K Thielemann, *Astrophys. J.* **363**, 340 (1990)
[3] J H Applegate, C J Hogan and R J Scherrer, *Astrophys. J.* **329**, 572 (1988)
[4] T Sasaqui *et al*, *Astrophys. J.* **634**, 1173 (2005)
[5] H Beer *et al*, *Astrophys. J.* **387**, 258 (1992)
[6] R Reifarth *et al*, *Phys. Rev. C* **77**, 015804 (2008)
[7] Á Horváth *et al*, *Astrophys. J.* **570**, 926 (2002)
[8] U Datta Pramanik *et al*, *Phys. Lett. B* **551**, 63 (2003)
[9] U Datta Pramanik *et al*, *J. Phys. G* **31**, S1583 (2005)

[10] T Nakamura *et al*, *Phys. Rev. C* **79**, 035805 (2009)
[11] C Rolfs, *Nucl. Phys. A* **217**, 29 (1973)
[12] H Herndl *et al*, *Phys. Rev. C* **60**, 064614 (1999)
[13] P Descouvemont, *Nucl. Phys. A* **675**, 559 (2000)
[14] N K Timofeyuk, D Baye, P Descouvemont, R Kamouni and I J Thompson, *Phys. Rev. Lett.* **96**, 162501 (2006)
[15] N C Summers and F M Nunes, *Phys. Rev. C* **78**, 011601(R) (2008)
[16] H Esbensen, *Phys. Rev. C* **80**, 024608 (2009)
[17] P Banerjee, R Chatterjee and R Shyam, *Phys. Rev. C* **78**, 035804 (2008)
[18] R Chatterjee, P Banerjee and R Shyam, *Nucl. Phys. A* **675**, 477 (2000)
[19] A Nordsieck, *Phys. Rev.* **93**, 785 (1954)
[20] R Shyam and M A Nagarajan, *Ann. Phys. (New York)* **163**, 265 (1985)
[21] R Chatterjee, *Phys. Rev. C* **68**, 044604 (2003)
[22] M Zadro, *Phys. Rev. C* **66**, 034603 (2002)
[23] C A Bertulani and G Baur, *Phys. Rep.* **163**, 299 (1988)
[24] J T Huang, C A Bertulani and V Guimarães, *Atomic Data Nucl. Data Tables* **96**, 824 (2010), arXiv:nucl-th/0810.3867
[25] G Baur, C A Bertulani and H Rebel, *Nucl. Phys. A* **458**, 188 (1986)
[26] A N F Aleixo and C A Bertulani, *Nucl. Phys. A* **505**, 448 (1989)
[27] M A Nagrajan, S Lenzi and A Vitturi, *Eur. Phys. J. A* **24**, 63 (2005)
[28] S Typel and G Baur, *Nucl. Phys. A* **759**, 247 (2005)
[29] R Chatterjee, L Fortunato and A Vitturi, *Eur. Phys. J. A* **35**, 213 (2008)
[30] http://www.nndc.bnl.gov; EXFOR database (X4 dataset-22995)
[31] T Kajino, G J Matthews and G M Fuller, *Astrophys. J.* **364**, 7 (1990)
[32] L H Kawano, W A Fowler, R W Kavanagh and R A Malaney, *Astrophys. J.* **372**, 1 (1991)
[33] C E Rolfs and W S Rodney, *Couldrons in the cosmos* (University of Chicago Press, Chicago, 1988)